JOURNAL OF THERMOPHYSICS AND HEAT TRANSFER
Vol. 25, No. 1, January–March 2011

Thermal Diffusivity and Thickness of Fouling in Heat-Exchanger Tube Using Photothermal Method

A. Adili* and C. Kerkeni†
Centre de Recherches et des Technologies de l'Energie, 2050 Hammam-Lif, Tunisian Republic
and
S. Ben Nasrallah‡
Ecole Nationale d'Ingénieurs de Monastir, 5019 Monastir, Tunisian Republic

DOI: 10.2514/1.51111

Practical applications of models developed by the research community to predict fouling accumulation in heat-exchanger tubes have been reviewed recently. In fact, the majority of the developed techniques of detection and measurement of fouling properties (such as thickness, equivalent thermal diffusivity, and thermal resistance) are sophisticated. In this work, an inverse problem based on the use of a genetic algorithm that mimics its principles from the process of the evolution described by Darwin is applied to identify the thickness, the equivalent thermal diffusivity of fouling developed onto the internal surface of a heat-exchanger tube, and the thermal resistance contact between the fouling deposits and the material with which the heat-exchanger tube is made. The experimental device using a photothermal method with a finite-width-pulse heat excitation is used. The experimental results show that the apparatus is feasible as a noninvasive method to obtain good results.

Nomenclature

a_i	=	equivalent thermal diffusivity, $m^2 \cdot s^{-1}$
e	=	thickness, m
h	=	heat transfer coefficient, $W \cdot m^{-2} \cdot K^{-1}$
P	=	matrix of population
p	=	Laplace parameter, s^{-1}
$Q(t)$	=	heat flux excitation, $W \cdot m^{-2}$
R	=	radius, m
R_c	=	thermal contact resistance, $K \cdot m^2 \cdot W^{-1}$
$S(\beta)$	=	fitness function
T_{measured}	=	measured temperature, K
T_1	=	calculated temperature on the front face, K
T_2	=	calculated temperature on the rear face, K
t	=	time, s
t_c	=	heating time, s
X_β	=	sensitivity coefficients matrix
Z_β	=	reduced-sensitivity matrix
β	=	vector of estimated parameters
θ_f	=	Laplace temperature on the front face of the sample, $K.s^{-1}$
θ_r	=	Laplace temperature on the rear face of the sample, $K.s^{-1}$
Φ	=	Laplace heat flux excitation, $W \cdot m^{-2} \cdot s^{-1}$
Ψ	=	heat flux density, $W \cdot m^{-2}$

I. Introduction

THE presence of fouling in heat-exchanger equipment represents additional costs to the industry in terms of additional energy and labor (Wei [1]). This phenomenon generally exists in nature and in most industrial processes, especially in the heat transfer process. Fouling is formed by a mixture of inorganic salts. In most cases, it is made of calcium salts: carbonate, sulphate, or phosphate. Because of their poor thermal conductivity and their good adherence to the walls, these mineral compounds decrease the heat transfer rate, reduce the water flow rate, and even shorten equipment life by corrosion (Tlili et al. [2]). Furthermore, the overall complexity and the lack of fundamental understanding of the processes leading to fouling have hindered the development of a general theoretical framework, which could have been used to interpret or predict different types of experimental results (Katta [3]). Therefore, many studies on the heat-exchanger fouling have been carried out in recent years. They are progressing in three directions: that is, fouling prediction, fouling monitoring, and fouling countermeasure (Lingfang et al. [4]).

Since fouling is not usually visible from the outside of the industrial processing equipment and can only be ascertained from significant effects such as pressure drop measurement, its thickness may not be accurately measured with conventional mechanical instruments, and in some cases it is determined by an expensive and destructive test. The development of a suitable nondestructive technique to measure the fouling-layer thickness in real time, under realistic operating conditions, is of great importance. A number of noninvasive techniques have been used to study fouling deposits since the 1970s. These techniques include the use of a radioisotope technique, microarray of semiconductors, high-speed video camera (Mackley and Sherman [5] and Wakeman [6]), microstrip monitoring technique (Root and Kaufman [7]), photothermal deflection method (Fujimori et al. [8]), and ellipsometry (Karlsson et al. [9]). Other techniques use the NMR microimaging (Yao et al. [10]), the laser beam captor, and ultrasonic measurements methods (Lynnworth [11]). In addition to these techniques, Muzychka [12] presented a general solution for the thermal spreading resistances in compound annular sectors. In this system, heat flows through a portion of the outer surface through two layers, having different thermal conductivities, to the interior surface, which is convectively cooled by a uniform film conductance (Muzychka [12]). This general solution depends on the dimensions of the system at hand and its thermal properties. A particular application of this solution is used in heat-exchanger tubes to study the effects of protective coatings or fouling-layer thickness on its thermal efficiency.

The results of these studies provided valuable information on fouling-layer thickness. However, in industry, the determination of this information (fouling thickness) must be in situ, nondestructive, in real time, and reproducible, and the experimental device should be robust, inexpensive, and easy to use. For these reasons, the use of the

Received 10 June 2010; revision received 2 September 2010; accepted for publication 3 September 2010. Copyright © 2010 by the American Institute of Aeronautics and Astronautics, Inc. All rights reserved. Copies of this paper may be made for personal or internal use, on condition that the copier pay the $10.00 per-copy fee to the Copyright Clearance Center, Inc., 222 Rosewood Drive, Danvers, MA 01923; include the code 0887-8722/11 and $10.00 in correspondence with the CCC.

* Laboratoire des Procédés Thermique, Route Touristique de Soliman, B.P. 95; ladiliali@yahoo.fr.
† Laboratoire des Procédés Thermique, Route Touristique de Soliman, B.P. 95.
‡ Laboratoire des Etudes des Systèmes Thermiques et Energétiques, Avenue Ibn El Jazzar, Route de Kairouan.

above-mentioned techniques is very limited because of their high costs and their use of sophisticated devices and theories. In this study, an inexpensive unsophisticated experimental apparatus based on a photothermal method is used to identify the thickness of a fouling layer developed onto the internal surface of a heat-exchanger tube. The method primarily consists of subjecting the front surface of a fouled heat-exchanger tube to a finite-width heat flux excitation using a halogen lamp. During and after the irradiation, the temperature response is measured on the front face using an infrared thermosensor. Secondarily, a mathematical model describing the temperature evolution on the front face is developed using the thermal quadrupoles formalism. The mathematical model is a function of the thickness of the fouling layer, its equivalent thermal diffusivity, the thermal resistance contact with the wall, the parameters related to the geometry and the heat exchange coefficients with the environment. The identification of these parameters consists of minimizing the residual of an objective function that expresses the sum square of the gap between the measured temperature and the calculated one. In this work, a genetic algorithm that is a random search process is used to minimize this objective function.

Results of the identification procedure show the efficiency of the developed genetic algorithm to identify the thickness of the fouling layer and its equivalent thermal diffusivity without requiring information on their initial values or the use of sophisticated devices. However, the practical aspects of the apparatus should be improved in future work.

II. System Description and Formulation of the Mathematical Model

A heat exchanger is a specialized device that assists in the transfer of heat from one fluid to the other. In some cases, the fluids may be in direct contact with each other. In other designs, a solid wall may separate the fluids and prevent their mixture. In a heat-exchanger tube, conduction is present not only through the tube wall, but also through the deposits accumulated on the wall surface because of fouling (Amin [13]) (Fig. 1). Consequently, the apparatus may undergo a decline in its ability to transfer heat. In fact, the additional fouling layer has a low thermal conductivity that increases the resistance to heat transfer and reduces the performance of heat-exchanger tube.

To determine the thickness e_2 of the fouling deposited layer, a mathematical model describing the front surface temperature evolution of a heat-exchanger tube that is subjected to a finite-width-pulse heat flux $Q(t)$ at $t = 0$ s [Eq. (1)] during a short time t_c, is developed (Fig. 2):

$$Q(t) = \begin{cases} \Psi & 0 \le t \le t_c \\ 0 & t > t_c \end{cases} \tag{1}$$

where Ψ is the amplitude of the finite-width-pulse heat flux.

The model assumes one-dimensional heat flux through a two-layer sample composed of the two materials, which are copper and fouling deposits of thicknesses e_1 and e_2, respectively.

To determine the temperature evolution of the heat-exchanger front face after being subjected to a finite-width-pulse heat flux, the thermal quadrupoles formalism is used. The method originates in the integral transform treatment of the heat equation (André et al. [14]).

Fig. 1 Photograph of fouled heat-exchanger tube.

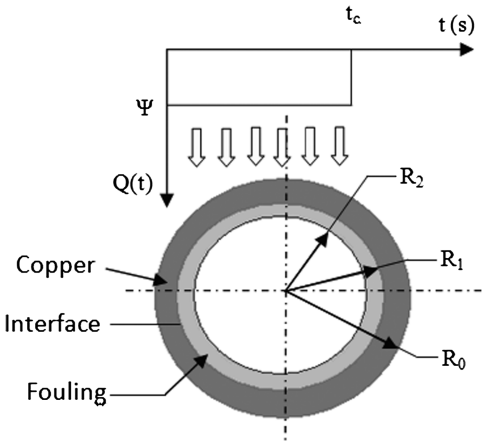

Fig. 2 Principle of the heat flux excitation with a finite width on the outside surface of the heat exchanger.

The method is considered applicable in only one direction and in a transient regime. Then one recovers an input–output matrix transfer formulation of the problem, well known from scientists working in the electronic field (automation systems) (André et al. [14]). The variables embedded in the formulation are the temperature (potential) and the heat flux (current) according to the well-known electrical analogy (André et al. [14]). For a material composed of one layer, the thermal quadrupole matrix is expressed as the following equation:

$$\begin{pmatrix} \theta_f \\ \phi_f \end{pmatrix} = \begin{pmatrix} A & B \\ C & D \end{pmatrix} \begin{pmatrix} \theta_r \\ \phi_r \end{pmatrix} \tag{2}$$

where A, B, C, and D are the coefficients of the quadrupole (their expressions depend on the Laplace variable p, the geometry, and the thermophysical properties of the material at hand), and θ and Φ represent the Laplace transforms of the temperature and the heat flux variables, respectively.

In this study, a transient heat flux is transferred through two layers. Each layer can be described by its own quadrupole matrix and the multilayered system can be modeled by multiplying the corresponding quadrupole matrix. The heat transfer into the two materials can be schematized, as shown in Fig. 3.

The thermal excitation of the system, which is composed of two isotrope layers, leads to a small temperature increase of about 2°C, so the thermal properties are considered constant and uniform. The convective and radiative heat transfers on the two faces with the uniform environment are expressed by two heat transfer coefficients h_1 and h_2, and the interface between the two materials is characterized by an imperfect contact (thermal contact resistance R_c). So according to Fig. 3, we can express the thermal quadrupoles between R_0 and R_2 and the boundary conditions as shown below.

First boundary condition, at $r = R_0$:

$$Q_0: \begin{bmatrix} \theta_f \\ \phi_f \end{bmatrix} = \begin{bmatrix} 1 & 0 \\ h_1 & 1 \end{bmatrix} \begin{bmatrix} \theta_0^1 \\ \phi_0^1 \end{bmatrix} \tag{3}$$

where $\phi_f = TL[Q(t)] = (\Psi/p)[1 - \exp(-pt_c)]$. For $R_0 < r < R_1$,

$$Q_{01}: \begin{bmatrix} \theta_0^1 \\ \phi_0^1 \end{bmatrix} = \begin{bmatrix} A_{01} & B_{01} \\ C_{01} & D_{01} \end{bmatrix} \begin{bmatrix} \theta_1^1 \\ \phi_1^1 \end{bmatrix} \tag{4}$$

Secondary boundary condition, at $r = R_1$:

$$Q_2: \begin{bmatrix} \theta_1^1 \\ \phi_1^1 \end{bmatrix} = \begin{bmatrix} 1 & R_c \\ 0 & 1 \end{bmatrix} \begin{bmatrix} \theta_1^2 \\ \phi_1^2 \end{bmatrix} \tag{5}$$

For $R_1 < r < R_2$,

$$Q_{12}: \begin{bmatrix} \theta_1^2 \\ \phi_1^2 \end{bmatrix} = \begin{bmatrix} A_{12} & B_{12} \\ C_{12} & D_{12} \end{bmatrix} \begin{bmatrix} \theta_2^2 \\ \phi_2^2 \end{bmatrix} \tag{6}$$

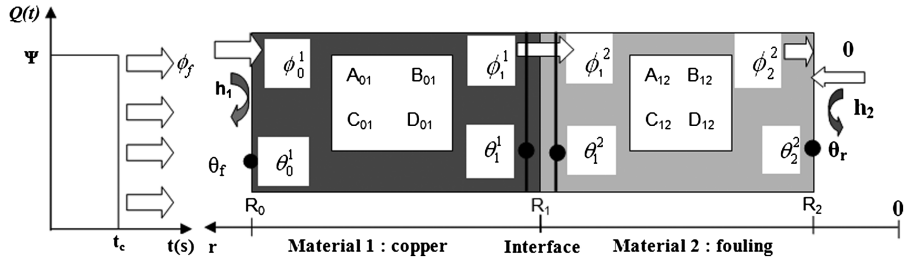

Fig. 3 Schematic presentation of the thermal quadrupoles.

Third boundary condition, at $r = R_2$:

$$Q_3: \begin{bmatrix} \theta_2^2 \\ \phi_2^2 \end{bmatrix} = \begin{bmatrix} 1 & 0 \\ h_2 & 1 \end{bmatrix} \begin{bmatrix} \theta_r \\ \phi_r = 0 \end{bmatrix} \tag{7}$$

Since the rear face is considered in adiabatic conditions and there is any source of heat flux, $\Phi_r = 0$.

The coefficients A_{ij}, B_{ij}, C_{ij} and D_{ij} depend on the Laplace parameter p, on the radius R_i of the layer i, and on the thermal diffusivities of the two materials. Their expressions are given by the following equations (Diaconu [15]):

$$A_{ij} = \alpha_j[I_0(\alpha_i)K_1(\alpha_j) + I_1(\alpha_j)K_0(\alpha_i)] \tag{8}$$

$$B_{ij} = \frac{\alpha_j}{q_j}[I_0(\alpha_j)K_0(\alpha_i) - I_0(\alpha_i)K_0(\alpha_j)] \tag{9}$$

$$C_{ij} = q_j\alpha_j[I_1(\alpha_j)K_1(\alpha_i) - I_1(\alpha_i)K_1(\alpha_j)] \tag{10}$$

$$D_{ij} = \alpha_j[I_0(\alpha_j)K_1(\alpha_i) + I_1(\alpha_i)K_0(\alpha_j)] \tag{11}$$

$$\alpha_{i,j} = q.R_{i,j}, \qquad q = \sqrt{\frac{p}{a_{i,j}}},$$
$$i = 0 \quad \text{or} \quad i = 1 \quad \text{and} \quad j = 1 \quad \text{or} \quad j = 2 \tag{12}$$

In this mathematical model, $\alpha_{i,j}$ has three expressions:

$$\alpha_0 = q_1.R_0 = \sqrt{\frac{p}{a_1}}R_0 \tag{13}$$

$$\alpha_1 = q_1.R_1 = \sqrt{\frac{p}{a_1}}R_1 \tag{14}$$

$$\alpha_2 = q_2.R_2 = \sqrt{\frac{p}{a_2}}R_2 \tag{15}$$

where a_1 is the equivalent thermal diffusivity of the copper with which the heat-exchanger tube is made; a_2 is the equivalent thermal diffusivity of the fouling deposited layer onto the internal surface of the heat-exchanger tube; I_0 and I_1 are the modified Bessel functions of the first kind and of the zero and first orders, respectively; and K_0 and K_1 are the modified Bessel functions of the second kind and of the zero and first orders, respectively.

The entire system can be described in Laplace space as

$$\begin{bmatrix} \theta_f \\ \frac{\psi[1-\exp(-pt_c)]}{p} \end{bmatrix} = \begin{bmatrix} 1 & 0 \\ h_1 & 1 \end{bmatrix} \begin{bmatrix} A_{01} & B_{01} \\ C_{01} & D_{01} \end{bmatrix} \begin{bmatrix} 1 & R_c \\ 0 & 1 \end{bmatrix} \begin{bmatrix} A_{12} & B_{12} \\ C_{12} & D_{12} \end{bmatrix} \begin{bmatrix} 1 & 0 \\ h_2 & 1 \end{bmatrix} \begin{bmatrix} \theta_r \\ 0 \end{bmatrix}$$
$$= \begin{bmatrix} A & B \\ C & D \end{bmatrix} \begin{bmatrix} \theta_r \\ 0 \end{bmatrix} \tag{16}$$

where θ_f and θ_r are the Laplace transforms of the front- and rear-face temperatures of the sample, respectively.

Using Eq. (16), the front-face temperature θ_f can be written as

$$\theta_f = A.\theta_r = \frac{\Psi}{p}\frac{A}{C}[1 - \exp(-pt_c)] \tag{17}$$

where A and C are given by the following equations:

$$A = A_{01}A_{12} + R_cA_{01}C_{12} + B_{01}C_{12} + h_2A_{01}B_{12} + h_2R_cA_{01}D_{12} + h_2B_{01}D_{12} \tag{18}$$

$$C = \delta + \varphi + \phi_1 + \phi_2 \tag{19}$$

where

$$\delta = C_{01}A_{12} + A_{01}C_{12} + R_cC_{01}C_{12} \tag{19a}$$

$$\varphi = h_1h_2[A_{01}B_{12} + R_cA_{01}A_{12} + B_{01}D_{12}] \tag{19b}$$

$$\phi_1 = h_1[A_{01}A_{12} + R_cA_{01}C_{12} + B_{01}C_{12}] \tag{19c}$$

$$\phi_2 = h_2[C_{01}B_{12} + R_cC_{01}D_{12} + A_{01}A_{12}] \tag{19d}$$

The front-face temperature $\theta_f(p)$ depends on several dimensional parameters. Some of these parameters are supposed to be known and the others will be identified. It is given by the following expression:

$$\theta_f(p) = f(p, t_c, a_1, a_2, R_0, R_1, R_2, h_1, h_2, R_c, \Psi) \tag{20}$$

The equivalent thermal diffusivity a_1 and the outside and inside radii (R_0 and R_1) of the first layer of copper with which the heat-exchanger tube is made are known. Moreover, the amplitude Ψ and the duration t_c of the heat flux excitation $Q(t)$ are known from other measurements. The remaining parameters that are given in the following vector $\beta = [a_2, R_2, h_1, h_2, R_c]$ are the parameters of interest. This vector β to be estimated includes the equivalent thermal diffusivity a_2 of the fouling layer, its inside radius R_2 (which is in the center of interest), the heat transfer coefficients on the two faces h_1 and h_2, and the thermal contact resistance R_c between the two layers.

To simplify the mathematical model presentation, the vector of the unknown parameters is written in the following form:

$$\beta = [\beta_1 = a_2,\ \beta_2 = R_2,\ \beta_3 = h_1,\ \beta_4 = h_2,\ \beta_5 = R_c]$$

The variation of the temperature $T_1(t, \beta)$ with time in the usual space domain is calculated using the numerical algorithm proposed by Graver–Stehfest of $\theta_r(p)$ (Albouchi et al. [16]):

$$T_1(t, \beta) = \frac{Ln(2)}{t}\sum_{i=1}^{n} V_i\theta_r\left(\frac{iLn(2)}{t}\right) \tag{21}$$

where V_i are the Graver–Stehfest coefficients function, and $\beta = [\beta_1, \beta_2, \beta_3, \beta_4, \beta_5]$ is the vector of the unknown parameters to be estimated using an inverse problem based on a genetic algorithm.

III. Sensitivity Study

A sensitivity study is a crucial step before starting any estimation procedure. In fact, it gives a useful piece of information that concerns both the magnitude of the parameters sensitivity coefficients and the degree of correlation between the unknown parameters. A sensitivity coefficients matrix X_β is defined as the effect that a change in a particular parameter β has on the variable state. Mathematically, it is defined as the first derivative of the measured variable with respect to the parameters of the model:

$$X_{\beta j} = \left.\frac{\partial T_1(t,\beta)}{\partial \beta}\right|_{\beta_j \neq \beta} \tag{22}$$

where $\beta = [\beta_1, \beta_2, \beta_3, \beta_4, \beta_5]$ and β_j are all parameters other than β that remain constant.

When performing a sensitivity study, it is important to examine the reduced sensitivities $Z_{\beta j}$, which are obtained by multiplying the original coefficients by the parameter referred to (Raynaud [17]). These coefficients have the same unit as the state variable (temperature). Using the finite difference approximation, the reduced-sensitivity coefficients are expressed as

$$Z_{\beta j} = \beta_j X_{ij} = \beta_j \frac{T_{i1}(t, \beta_j + \delta\beta) - T_{i1}(t, \beta_j)}{\delta\beta_j} \tag{23}$$

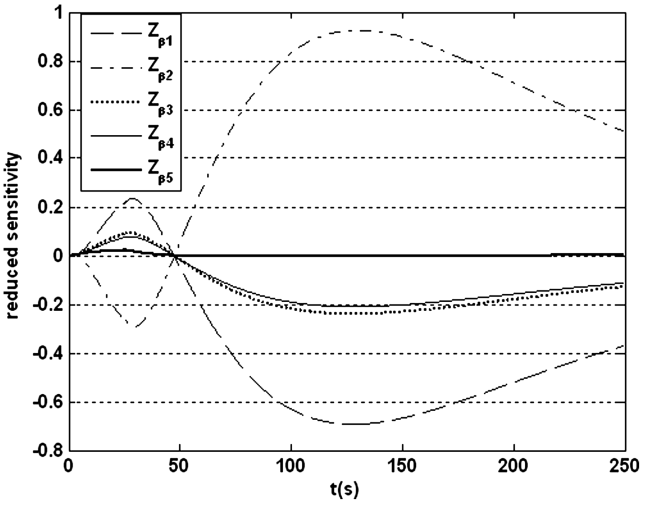

Fig. 4 Variation of the reduced sensitivities of the unknown parameters of the mathematical model.

where $\delta\beta = (0, \ldots, 0, \delta\beta, 0, \ldots, 0)$ is a small variation of the parameter β_j.

If the reduced-sensitivity coefficients do not depend on each other over the range of the observations, then the estimation is said to be linear and the parameters are uncorrelated. It is extremely important to determine whether the parameters to be estimated are correlated or not. In fact, if they are correlated or nearly correlated, they cannot be estimated simultaneously.

According to Fig. 4, which shows the variation of the reduced sensitivities of the five parameters versus time, we note that the mathematical model is very sensitive to the equivalent thermal diffusivity a_2, the inside radius R_2, and the heat transfer coefficients on the two faces h_1 and h_2, whereas it is less sensitive to the thermal contact resistance R_c. Thus, we can say that this last parameter will be estimated with a low accuracy.

Furthermore, Fig. 4 shows that the reduced-sensitivity coefficients of the equivalent thermal diffusivity a_2 and the inside radius R_2 have the same shape and their maxima are reached almost at the same time; in addition, Fig. 5a shows that these two parameters are strongly correlated. Moreover, it can be seen from Fig. 4 that the reduced-sensitivity coefficients of h_1 and h_2 are linearly dependent. This remark can be emphasized by Fig. 5b, which shows that in most cases h_1 and h_2 are linearly, positively, and perfectly correlated, which indicates that they cannot be simultaneously identified. Consequently, correlation between these parameters is precious information that leads us to choose the adequate parameters estimation procedure. In fact, a bad choice of the parameters estimation procedure can show instabilities resulting in nonconvergence if two or more than two parameters are correlated or nearly correlated.

IV. Estimation of the Unknown Parameters by Means of a Genetic Algorithm

The main goal of the estimation procedure is to find the values of the unknown parameters of the vector β that minimize the sum of the squared residuals between the measured temperature T_{measured} and the mathematical model output $T_1(t, \beta)$ as it is written in the following equation:

$$\min(S(\beta)) = \min\left(\sum_{i=1}^{N} (T_{\text{measured}} - T_1(t,\beta))^2\right) \tag{24}$$

In this parameters estimation process, the inside radius R_2 and the equivalent thermal diffusivity of the developed fouling layer are the main parameters of interest, the others are additional parameters.

There are many methods to minimize this objective function, $S(\beta)$, among them we mention gradient methods that are largely used by many researchers in different domains. Although these techniques

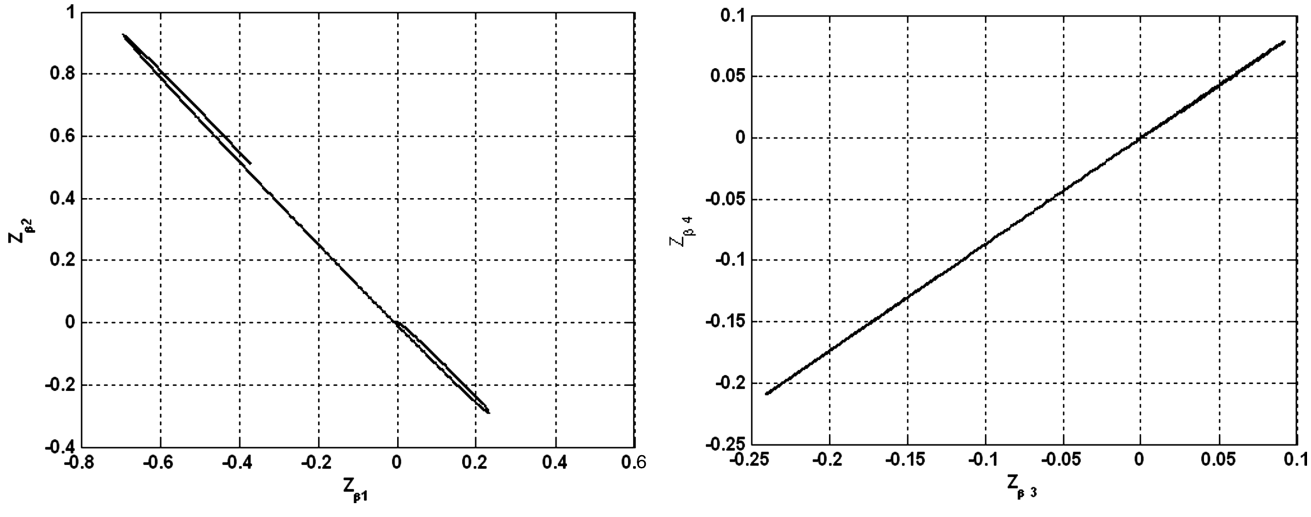

a) b)

Fig. 5 Linear dependence between the dimensionless sensitivity coefficients of 1) $Z_{\beta 1}$ and $Z_{\beta 2}$ and b) $Z_{\beta 4}$ and $Z_{\beta 3}$.

are well developed, they maintain significant drawbacks. Their principle requires the evaluation of the derivatives of the objective function $S(\beta)$ by differentiating Eq. (24) with respect to each of the unknown parameters β_j $(j = 1, \ldots, 5)$ and then setting the resulting expression equal to zero, yielding to the following set of algebraic equations:

$$\sum_{i=1}^{n} 2^* \frac{\partial T_1(t,\beta)}{\partial \beta_j}[T_1(t,\beta) - T_{\text{measured}}] = 0 \qquad (25)$$

From their principles, we note that gradient methods can be applicable only for derivable functions. Furthermore, employing gradient search methods need to start from an initial guessed solution near the exact solution. In these approaches, the use of a bad starting point may result in the solution getting trapped in a local optimum (Tamer et al. [18]). In addition, the sensitivity study has shown that more than two parameters are strongly correlated, which is a limiting factor to use gradient methods as estimation parameter procedures. Consequently, we are in need of a procedure that allows us to estimate the unknown parameters of the vector β even in the presence of a strong correlation between them, without the necessity of working with gradients and without requiring information on an initial solution. Therefore, in the solution of the inverse problem, genetic algorithms are the most widely used optimization methods that can be advantageously used for many optimization problems. In this study, a genetic algorithm is implemented to search for the optimal values of the vector β composed of five parameters $[\beta_1, \beta_2, \beta_3, \beta_4, \beta_5]$, called chromosomes or individuals, that give the mathematical model output $T_1(t, \beta)$ sufficiently close to the measurements T_{measured}.

A genetic algorithm is a stochastic search algorithm that imitates its basic principles from natural selection and survival mechanism of the fittest from natural evolution, which were first described by Darwin. Genetic algorithm became popular in the early 1970s through the work of Holland [19]. Differing from conventional search techniques, a genetic algorithm starts randomly with an initial generated population of solutions of n individuals [Eq. (26)] satisfying boundaries and system constraints:

$$P = \begin{bmatrix} \beta_1^1 & \beta_2^1 & \beta_3^1 & \beta_4^1 & \beta_5^1 \\ \beta_1^2 & \beta_2^2 & . & . & \beta_5^2 \\ . & . & . & . & . \\ . & . & \beta_3^j & . & . \\ \beta_1^n & \beta_2^n & \beta_3^n & \beta_4^n & \beta_5^n \end{bmatrix} = \begin{bmatrix} \beta^1 \\ \beta^2 \\ . \\ . \\ \beta^n \end{bmatrix} \qquad (26)$$

Each row in the population P is called a chromosome or individual, representing a solution to the problem at hand. A chromosome is a full set of the unknown parameters of the vector β. Optimal parameters are obtained by exchanging genetic information between individuals to reproduce improved solutions from one generation to the next by three genetic operators, which are selection, crossover, and mutation (Fig. 6):

The chromosome evolves through successive generations. During each generation, every chromosome is evaluated by measuring its fitness in the population and assigning to it a score. In this study, the fitness function is equal to the objective function. To create the next generation, new chromosomes, called offspring or children, are formed by either merging two chromosomes from the current generation using a crossover operator or modifying a chromosome using a mutation operator. The crossover operator takes two selected individuals and combines them about crossover points thereby creating two new individuals. The mutation operator randomly modifies the genes β_i^j of a chromosome β^j, introducing further randomness into the population. A new generation is formed by selection, according to the fitness values, some of the best parents and offspring are kept, the others are rejected to keep the population size constant. Fitter chromosomes have higher probabilities of being selected. After several generations, the algorithm converges to the

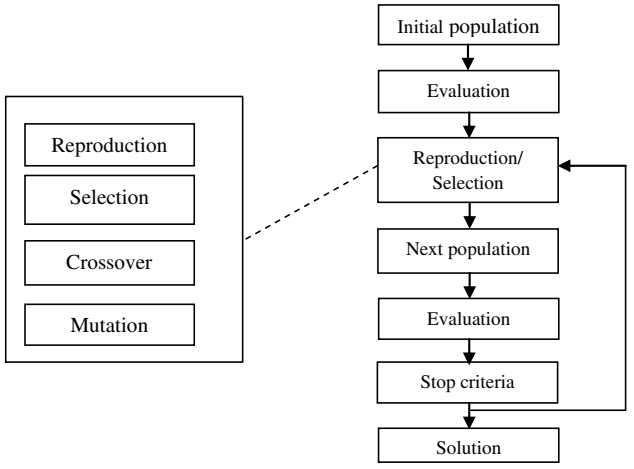

Fig. 6 Genetic algorithm flowchart.

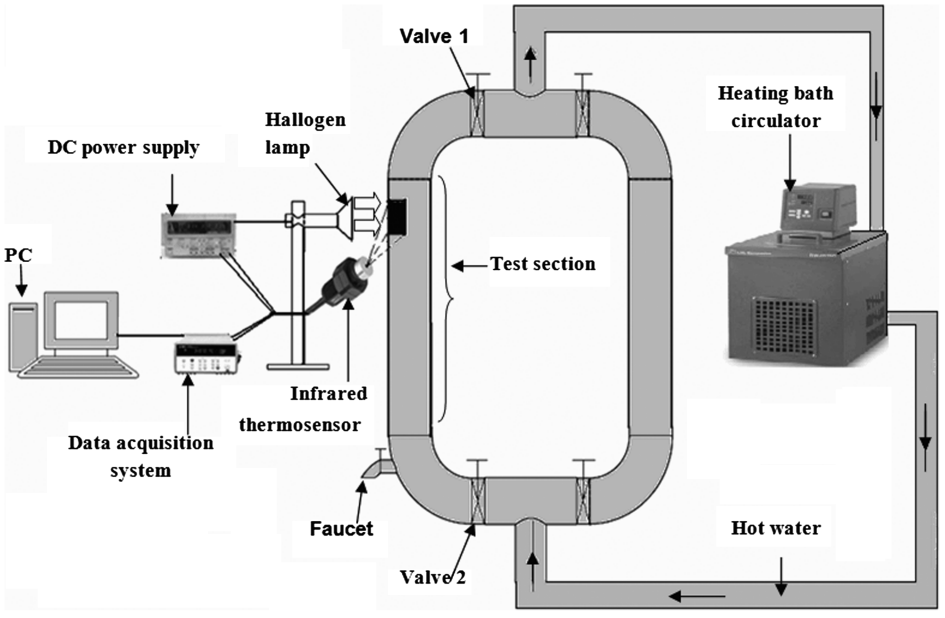

Fig. 7 Experimental apparatus.

Table 1 Fixed parameters for the estimation

Parameters	Values
Equivalent thermal diffusivity a_1 of copper, $m^2 \cdot s^{-1}$	116×10^{-6}
Outside radius of copper, mm	7
Inside radius of copper, mm	6
Heat flux amplitude Ψ, $W \cdot m^{-2}$	1000
Heat flux duration t_c, s	15

best chromosome, which is anticipated to represent the optimum or suboptimal solution that gives the most minimal fitness function.

V. Experimental Setup and Results

The principal constituents that cause fouling deposits are calcium sulphate and calcium carbonate. Because of the slow process of fouling, most studies have been conducted on accelerated fouling using a very high foulant concentration (Qingjun et al. [20]). This allows significant fouling to occur within several hours or days. In this work, the calcium sulphate (CaSO4) is used as a solute and is pumped into the flow channel that is made of copper using a heating-bath circulator (20 liters), which heats up the fluid temperature to 80°C (Fig. 7).

Before the fluid enters in the test section of 2 m length, there is a 2.8-m-long flow channel before the test section to ensure that a well-developed laminar flow was established. The fluid leaving the flow channel returned to the heating-bath circulator.

Qingjun et al. [20] demonstrated that the flow velocity of cooling water within heat-exchanger tubes has major influences on the asymptotic fouling resistance as well as the suspension rate. For this reason, the velocity of the liquid flow was kept at $0.025\ m \cdot s^{-1}$, corresponding to a Reynolds number of 695. This low Reynolds number accelerates the accumulation of the fouling deposits onto the internal surface of the heat-exchanger tube, since the deposits removal rate was minimized. The fluid was left circulating for 5 h to ensure the fouling deposition onto the internal surface of the flow channel. After which, valves 1 and 2 were turned off and the fluid was drained out of the test section through a faucet and returned to the heating-bath circulator.

To identify the thickness of the deposited fouling layer and the values of the unknown thermophysical properties of the vector β, an imposed heat flux with a finite-width was applied across the front surface of the test section using a halogen lamp (Fig. 7), which provides a uniform heat flux equal to $1\ kW \cdot m^{-2}$, during 15 s. To increase and to make a uniform absorption, the front surface of the test section was coated with a thin layer of black paint.

The identification procedure consists of minimizing the objective function that gives the sum of the squared residuals between the mathematical model output given in Eq. (17) and the measured temperature $T_{measured}$ at the front surface of the test section. So an infrared thermosensor located at the front surface of the test section (Fig. 7) is used to measure the temperature evolution during and after the absorption of the heat flux density delivered by the halogen lamp. The measurement is performed for 250 s, and the sampling interval is set as 0.25 s throughout the entire temperature recording. After the thermal excitation, the temperature of the front surface of the test section reaches a maximum and then decreases due to the heat diffusion. The electrical signal, being proportional to the temperature variation $T_{measured}$ and depending on the various unknown parameters of the vector β to be identified, is read and recorded with a data acquisition unit (Agilent 34970A), which allows transferring data to a computer via an RS-232 interface.

In this identification procedure of the unknown parameters, the values of the equivalent thermal diffusivity a_1, the outside and inside radii (R_0 and R_1) of the first layer of copper with which the heat-exchanger tube is made of, the amplitude Ψ and the duration t_c of the heat flux excitation $Q(t)$ are fixed and summarized in Table 1.

The estimation is carried on with a genetic algorithm with a population of 100 chromosomes, each one of five genes (the five unknown parameters of the vector β), and in 200 generation steps with the same procedure. The initial population is generated in a large domain. Each parameter β_i is delimited by an upper and a low bound: that is, $a_2 \in [10^{-7}, 10^{-5}\ m^2 \cdot s^{-1}]$, $R_2 \in [0, 6\ mm]$, $h_1 \in [1, 25\ W \cdot m^{-2} \cdot K^{-1}]$, $h_2 \in [1, 25\ W \cdot m^{-2} \cdot K^{-1}]$, $R_c \in [10^{-6}, 10^{-3}\ K \cdot m^2 \cdot W^{-1}]$.

Figure 8 shows a comparison between the measured temperature and the calculated one using 10 chromosomes of the initial population. According to this figure, we notice that these initial chromosomes are not potential solutions, but the importance is that they must just provide an answer until this stage, even a poor one.

The rank-based selection is used in this algorithm. The new population is chosen from the old based on the rank: the highest-fitness member in the old population is ranked no. 1, the second-best solution is ranked no. 2, etc. In the new population of size 50 chromosomes, 80% of chromosomes are chosen from the top 40% of the old population, and the other 20% are chosen from the bottom 80%. This ensures that the selective operator maintains the genetic diversity. Then the three-point crossover is used; its technique is illustrated in Fig. 9. Three points are chosen along the length of the chromosome, and the parameters between those three points are then swapped on each parent chromosome to make two new children.

Finally, to satisfy the diversity of the population, every individual is subject to a random change by the mutation operator (Fig. 10).

This iterative process (evaluation, selection, crossover, and mutation) is stopped when the fitness function of the best

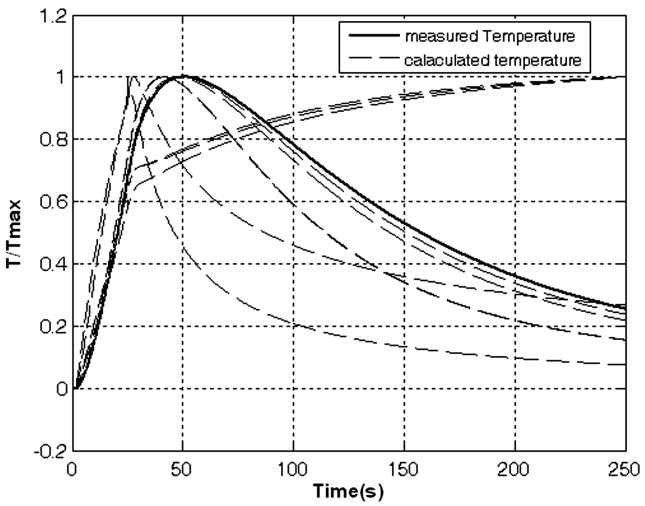

Fig. 8 Comparison between the measured temperature and the calculated temperature for the initial population.

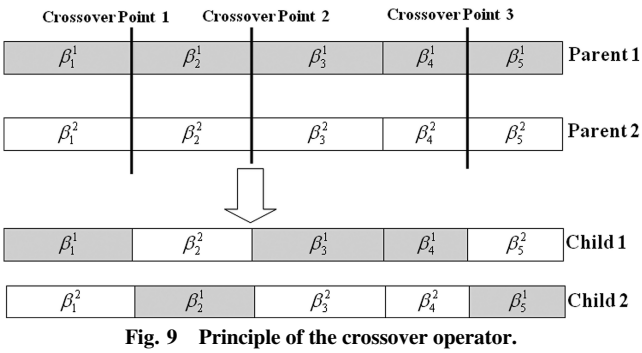

Fig. 9 Principle of the crossover operator.

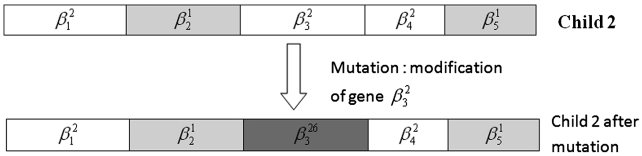

Fig. 10 Principle of the mutation operator.

Table 2 Estimated parameters

Parameters	Values	Standard deviation σ
a_2, $m^2 \cdot s^{-1}$	0.97×10^6	0.072×10^6
R_2, mm	5.08	0.07
h_1, $W \cdot m^{-2} \cdot K^{-1}$	14.6	1.29
h_2, $W \cdot m^{-2} \cdot K^{-1}$	13.2	1.02
R_c, $K \cdot m^2 \cdot W^{-1}$	2.04×10^5	0.842×10^5

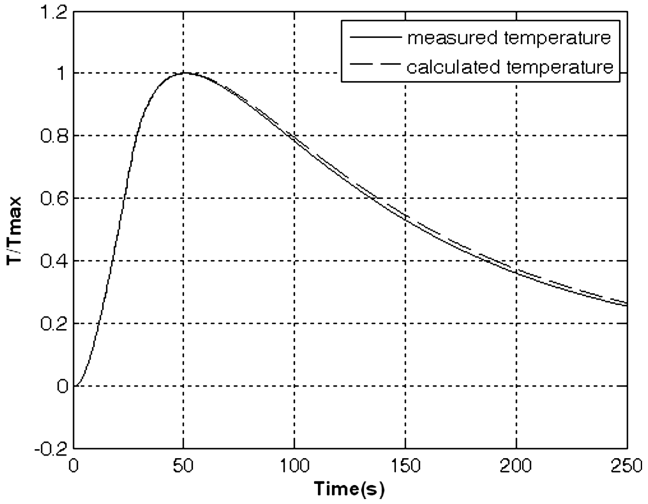

Fig. 11 Comparison between the measured and the calculated temperatures at the convergence of the genetic algorithm.

chromosome is lower than 10^{-3} K^2 and the algorithm achieves 200 generations. The performance of the genetic algorithm was performed by averaging 10 runs with different initial populations. The genetic algorithm converges to the average parameters given in Table 2. The results indicate that the developed genetic algorithm allows the simultaneous estimation of the unknown parameters of the vector β. The quality of the estimation procedure is analyzed by comparing the measured temperature and the calculated one using the best chromosomes estimated by the genetic algorithm. Figure 11 presents a comparison between the measurements and the optimal model using the estimated parameters. It shows that the obtained parameters give a mathematical model output $T_1(t, \beta)$ sufficiently close to the measured temperature T_{measured}.

We notice that the estimated radius R_2 of the fouling deposited at the inlet of the test section, given in Table 2, is obtained after 5 h of circulation of the fluid in the flow channel. In fact, the accumulation rate of fouling increases with time.

The thickness ($e_2 = R_1$–R_2) of the developed layer of fouling at the inlet of the test section is deduced from the gap between the inside radius R_1 of the heat-exchanger tube and the estimated radius R_2 of the fouling deposited layer. To qualify the value of the estimated radius, the thickness of the fouling deposits at the inlet of the test section is measured using a digital caliper that has a rated accuracy of 0.01 mm. The comparison between the measured and the calculated thickness is summarized in Table 3.

These results show that the proposed solution is effective in the determination of the unknown properties of the fouling accumulated onto the internal surface of the heat-exchanger tube, the heat exchange coefficients, and the thermal resistance contact. It should

Table 3 Comparison between the measured and the calculated thickness of the fouling layer

Parameters	Values
Calculated thickness $e_2 = R_1$–R_2, mm	0.92
Measured thickness, mm	0.93

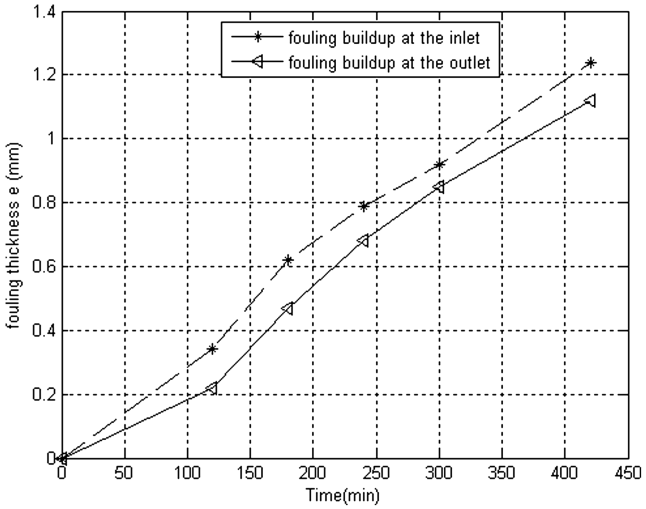

Fig. 12 Evolution of the fouling buildup at the inlet and outlet of the test section.

be emphasized that one of the advantages of the proposed algorithm is that there is no need to define an initial solution to start the optimization process.

The deposit growth during the fouling buildup onto the internal surface of the test section has been studied in this work. Figure 12 shows a comparison between the evolution of the estimated thickness of the fouling layer at different times at the inlet and outlet of the test section. Each point of the two curves is obtained by repeating the experience using the same operating conditions.

According to Fig. 12, we note a dramatic increase of the fouling layer after 420 min and a nonuniform distribution of the fouling deposited along the test section. Typically, the fouling thickness at the inlet and outlet was about 0.34 and 0.22 mm, respectively, after 120 min and about 1.24 and 1.12 mm, respectively, after 420 min. The formation of a nonuniform fouling layer is due to the fact that the temperature at the inlet of the test section is a bit higher than the temperature at the outlet of the test section as a result of the heating-bath circulator.

VI. Conclusions

This study demonstrates the interest of the photothermal method associated with a genetic algorithm, as a stochastic search, to detect and to estimate the thickness and the equivalent thermal diffusivity of the fouling deposited onto the internal surface of a heat-exchanger tube. The nongradient nature of genetic algorithms has been exploited to handle problems of initialization and correlation between parameters.

On one hand, the results of the estimation method show the ability of the photothermal method to be used as a noninvasive method to detect the fouling buildup. This technique has the potential to measure the thickness of fouling deposits onto a surface of a heat-exchanger tube. On the other hand, the results show the power of the developed genetic algorithm to estimate a large number of parameters even in the presence of a strong correlation between them.

References

[1] Wei, L. "Energy Penalty Associated with Fouling in Enhanced Tubes in Chiller-Flooded Condenser," *8th AIAA/ASME Joint Thermophysics and Heat Transfer Conference* [CD-ROM], AIAA, Reston, VA, 24–26 June 2002.

[2] Tlili, M. M., Rousseau, P., Ben Amor, M., and Gabrielli, C. "An Electrochemical Method to Study Scaling by Calcium Sulphate of a Heat Transfer Surface," *Chemical Engineering Science*, Vol. 63, 2008, pp. 559–566.
doi:10.1016/j.ces.2007.09.035

[3] Katta, V. R. "Numerical method for simulating fluid-dynamic and heat-transfer changes in jet-engine injector feed-arm due to fouling," *Journal of Thermophysics and Heat Transfer*, Vol. 7, No. 4, 1993, pp. 651–660.

doi:10.2514/3.474

[4] Lingfang, S., Yingying, Z., Xinpeng, Z., Shanrang, Y., and Yukun, Q. "Research on the Fouling Prediction of Heat Exchanger Based on Support Vector Machine," *Proceedings of the International Conference on Intelligent Computation Technology and Automation ICICTA*, 2008, pp. 240–244.

[5] Mackley, M. R. and Sherman, N. E. "Cross-Flow Cake Filtration Mechanisms and Kinetics," *Chemical Engineering Science*, Vol. 47, 1992, pp. 3067–3084.
doi:10.1016/0009-2509(92)87007-D

[6] Wakeman, R. J. "Visualization of Cake Formation in Cross Flow Microfiltration," *Transactions of the Institution of Chemical Engineers*, Vol. 72, 1994, Pt. A, pp. 530–540.

[7] Root, L. F., and Kaufman, I. "Non-Contacting Low-Cost Instrument for Film Thickness Measurement," *IEEE Transactions on Instrumentation and Measurement*, Vol. 41, 1992, pp. 1014–1019.
doi:10.1109/19.199384

[8] Fujimori, H., Asakura, Y., and Suzuki, V. "Non-Contact Measurement of Film Thickness by the Photothermal Deflection Method," *Japanese Journal of Applied Physics*, Vol. 26, 1987, pp. 1759–1764.
doi:10.1143/JJAP.26.1759

[9] Karlsson, C. A. C., Wahlgren, M. C., and Tragardh, A. C. "Betalactoglobulin Fouling and Its Removal Upon Rinsing and by SDS as Influenced by Surface Characteristics, Temperature and Adsorption Time," *Journal of Food Engineering*, Vol. 30, 1996, pp. 43–60.
doi:10.1016/S0260-8774(96)00045-3

[10] Yao, S., Costello, M., Fane, A. G., and Pope, J. M. "Noninvasive Observation of Flow Profiles and Polarization Layers in Hollow Fibre Membrane Filtration Modules Using NMR Microimaging," *Journal of Membrane Science*, Vol. 99, No. 3, 1995, pp. 207–216.
doi:10.1016/0376-7388(94)00219-O

[11] Lynnworth, L. C. *Ultrasonic Measurement for Process Control Theory, Techniques, Applications*, Academic Press, San Diego, CA, 1989.

[12] Muzychka, Y. S. "Thermal Spreading Resistances in Compound Annular Sectors," *Journal of Thermophysics and Heat Transfer*, Vol. 15, No. 3, 2001, pp. 354–359.
doi:10.2514/2.6615

[13] Amin, M. R. "Conjugate Forced Convection Heat Transfer in Tubes with Obstruction," *Journal of Thermophysics and Heat Transfer*, Vol. 12, No. 1, 1998, pp. 114–116.
doi:10.2514/2.6311

[14] André, S., Rémy, B., Pereira, F. R., Cella, v., and Silva Neto, A. J. "Hot Wire Method for the Thermal Characterization of Materials: Inverse Problem Application," *Engenharia Térmica*, Vol. 4, 2003, pp. 55–64.

[15] Diaconu, G. "Contribution à l'Optimisation des Revêtements des Moules de Fonderie: Application aux Outillages de Coulée Centrifuge," Ph.D. Thesis, Institut National Polytechnique de Toulouse, Centre de Recherche Outillages Matériaux et Procédés, Toulouse, France, 2004.

[16] Albouchi, F., Fetoui, M., Rigollet, F., Sassi, M., and Ben Nasrallah, S. "Optimal Design and Measurement of the Effective Thermal Conductivity of a Powder Using a Crenel Heat Excitation," *International Journal of Thermal Sciences*, Vol. 44, 2005, pp. 1090–1097.
doi:10.1016/j.ijthermalsci.2005.04.003

[17] Raynaud, M. "Strategy for Experimental Design and the Estimation of Parameters," *High Temperatures-High Pressures*, Vol. 31, 1999, pp. 1–15.
doi:10.1068/htps7

[18] Tamer, A. M., Halil, K., and Mustafa, A. M. "Aquifer Parameter and Zone Structure Estimation Using Kernel-Based Fuzzy C-Means Clustering and Genetic Algorithm," *Journal of Hydrology*, Vol. 343, 2007, pp. 240–253.
doi:10.1016/j.jhydrol.2007.06.018

[19] Holland, J., *Adaptation in Natural and Artificial Systems*, Univ. of Michigan Press, Ann Arbor, MI, 1975.

[20] Qingjun, K., Jinping, L., and Xuefeng, L. "Effect of Flow Conditions on Particulate Fouling in Shell-and-Tube Heat Exchangers," *8th AIAA/ASME Joint Thermophysics and Heat Transfer Conference* [CD-ROM], AIAA, Reston, VA, 24–26 June 2002.